Probing the local electronic structure of the cross-linked (1×2) reconstruction of rutile TiO$_2$(110)

Chi Ming Yim, Chi Lun Pang, Geoff Thornton*

Department of Chemistry and London Centre for Nanotechnology, University College London, 20 Gordon Street, London, WC1H 0AJ, UK

*Corresponding Author. E-mail: g.thornton@ucl.ac.uk

Keyword: Tunneling spectroscopy; titanium dioxide; reconstruction

The electronic structure of cross-linked TiO$_2$(110)-(1×2) has been investigated using scanning tunneling spectroscopy (STS) and by monitoring changes in ultraviolet photoelectron spectroscopy (UPS) following exposure of the surface to O$_2$. STS reveals two states located in the bandgap, at 0.7 and 1.5 eV below the Fermi level. The population of these two states varies over different parts of the (1×2)-reconstructed surface. An addition state at 1.1 eV above the Fermi level is observed at the double link part of the structure. All of the bandgap states are attenuated following exposure to O$_2$, while the workfunction is increased. We attribute this to an electron transfer from the surface to the adsorbed oxygen.

Introduction

Titanium dioxide (TiO_2) finds many uses such as in photocatalysis, heterogeneous catalysis, light harvesting, and gas sensing [1-3]. Among all facets of different TiO_2 polymorphs, the (110) face of TiO_2 rutile is the most stable [1], and has been widely investigated. Depending on the level of reduction of the TiO_2 bulk, the TiO_2(110) surface can undergo various surface reconstructions, most notably a simple (1×2) phase [4,5], a cross-linked (1×2) phase [5,6], as well as a pseudo-hexagonal rosette structure [7].

The geometric and electronic structure of bulk-terminated TiO_2(110)-(1×1) is well understood [1,3]. However, the picture is not yet clear for other surface terminations. For the simple (1×2) reconstruction, several models have been proposed. The most commonly accepted structure is the added Ti_2O_3 model, which consists of added Ti_2O_3 units on the (1×1) face [8]. This assignment is supported by quantitative low energy electron diffraction LEED-$I(V)$ measurement [4,9]. Several other models have been proposed, including most recently an added Ti_2O model proposed by Park *et al.* [10] that is favored in a transmission electron microscopy (TEM) study [11].

Several models have also been proposed for the cross-linked (1×2) reconstruction, including the same added Ti_2O_3 model [12] and an added Ti_3O_6 model [5,13]. While the added Ti_3O_6 model is supported by a non-contact atomic force microscopy measurement [6], Wang *et al.* [14] point out that the structure of the cross-linked (1×2) phase should be less stoichiometric than the simple (1×2) reconstruction, and instead propose a Ti_3O_2 model.

While there have been numerous studies of the geometric structure of the (1×2) reconstructions, the electronic structure has received less attention. An early photoemission spectroscopy study showed that the $TiO_2(110)$ surface with a (1×2) reconstruction exhibits a much more intense band-gap-state (BGS) peak than the $TiO_2(110)$-(1×1) surface [15]. This was corroborated by an ultraviolet photoelectron spectroscopy (UPS) study by Sánchez-Sánchez et $al.$ [16], which shows that the BGS peak is composed of two individual components: a major peak located at a binding energy (BE) ~0.75 eV below the Fermi level (E_F) assigned to Ti^{3+} species associated with the point defects in the TiO_2 bulk and a minor peak located ~1.2 eV below E_F assigned to Ti_2O_3 rows.

Room temperature scanning tunneling spectroscopy (STS) has also been employed to probe the local electronic structure of the (1×2) surface [17,18]. Murray et $al.$ [17] detected a peak at about -1.5 V in a differential conductance spectrum of cross-linked (1×2). Batzill et $al.$ [18] detected a similar peak (at -1.6 V) as well as one at -1 V in differential conductance spectra taken from strands of the simple (1×2) reconstruction. The peak at -1.6 V was assigned to the (1×2) row and that at -1 V was assigned to defects in the band gap with the same origin as the peak found in UPS for lightly reduced $TiO_2(110)$. These two peaks presumably correspond to the minor and major peaks in the work of Sánchez-Sánchez et $al.$ [16].

Here, we employ spatially-resolved STS at 78 K to probe the electronic structure of the cross-linked (1×2) structure. Broadly consistent with the measurements of Batzill et $al.$ [18], we find peaks in differential conductance spectra at -1.5 and -0.7 V. The high spatial resolution of our measurements allows us to show how the intensity of these peaks varies across the surface. In addition to this, UPS is used to investigate the effect on the electronic structure of the cross-linked $TiO_2(110)$-

(1×2) surface occasioned by exposure to O_2: the BGS peak is attenuated along with an increase in the surface workfunction.

Experimental

The experiments were carried out using an *Omicron GmbH* low temperature STM housed in an ultrahigh vacuum (UHV) system (base pressure = 2×10^{-11} mbar). The adjoining preparation chamber (base pressure = 2×10^{-10} mbar) was equipped with facilities for sample sputtering and annealing as well as low energy electron diffraction (LEED), X-ray photoelectron spectroscopy (XPS), and UPS.

The cross-linked $TiO_2(110)$-(1×2) surface was prepared with cycles of argon ion sputtering (1 kV) and annealing at 1100 K in vacuum until a well-ordered $TiO_2(110)$-(1×2) diffraction pattern was observed in LEED and any impurities were below the detection limit XPS. O_2 (99.996 %, *Laborgasse*) was dosed at a sample temperature of 300 K. For UPS measurement, O_2 was dosed into the preparation chamber by backfilling via a leak valve, while for STM, it was dosed onto the sample in the STM stage via a directional doser placed ~50 mm away from the sample.

He I (hv = 21.2 eV) UPS spectra were taken at normal emission with a pass energy of 9 eV. The workfunction Φ was measured by means of photo-induced secondary electron emission from the surface that was negatively biased (-V) [19]:

$$\Phi = E_0^{kin} + \Phi_{SP} + eV \quad (1)$$

where Φ_{SP} is the workfunction of the energy analyzer (which stays constant throughout the measurements) and E_0^{kin} the onset energy of the secondary electron emission spectra.

STM images associated with the STS measurements were taken in the constant current mode at 78 K. Images connected with O_2 adsorption were recorded

4

at 300 K. In all cases, electrochemically-etched tungsten tips were used. The tips were initially conditioned by annealing to 400 K, then with in-situ electrical pulses. STS measurements were recorded in the current-imaging tunneling spectroscopy (CITS) mode with an *I-V* curve recorded from every point of the simultaneously recorded STM images with 100×100 pixels. Ten thousand *I-V* curves were obtained in a 5×5 nm^2 region of the cross-linked $TiO_2(110)$-(1×2) surface. The *I-V* curves were collected at sample bias (V_{SAMPLE}) between +1.6 V and -2.4 V with increments of 0.1 V at a set point of +0.9 V and 0.15 nA.

To analyze the CITS data, we averaged approximately 50 tunneling spectra recorded for each feature of interest. Using these averaged *I-V* curves, the normalized conductance curve $\frac{dI/dV}{I/V}$ vs V or $\sigma(V)$ was plotted numerically and is representative of the local density of states (LDOS). Note that by definition [20], $\sigma(V)$ equals unity at $V = 0$.

Results and Discussions

Appearance of cross-linked (1×2) reconstruction in STM

Figure 1a shows a STM image taken from the as-prepared, cross-linked $TiO_2(110)$-(1×2) surface. The (1×2) strands are inter-connected by cross-links, mainly double links and occasionally single links. A higher resolution image is shown in Fig. 1(b) where it can be seen that each of the (1×2) strands consists a central row and two side rows each running along the [001] direction of the surface. On each row, the periodicity is 3 Å along [001], equal to the size of the (1×1) unit cell of $TiO_2(110)$ in this direction [1]. The protrusions on the central row are offset from

those along the side rows by half a unit (1.5 Å), thus giving rise to a rhombus configuration. As for the double-link, it consists of one brighter and one less bright spot at its center, as well as four bright spots at its corners.

CITS on the cross-linked (1×2) reconstruction of rutile TiO$_2$(110)

Tunneling spectroscopy measurements in the CITS mode were taken from the same area as that in Fig. 1b (see Movie S1). Alongside each set of CITS spectroscopy data, a topographic STM image is also recorded simultaneously. The CITS spectra can be thought of as a stack of tunneling current (I_T) maps recorded at different sample biases (V_{SAMPLE}) and any feature in the current maps can be correlated with the simultaneously recorded STM image as shown in Fig. 2a and b.

Fig. 2c displays a normalized conductance curve, $\sigma(V)$, which is an average of all the curves recorded over the surface region in Fig. 2a during CITS. This curve exhibits two peaks, one at sample bias (V_{SAMPLE}) of -0.7 V and another at -1.5 V in the filled state region, as well as a plateau that starts at +0.7 V in the empty state region.

Figs. 2d-f show $\sigma(V)$ curves recorded from specific features of the cross-linked (1×2) reconstruction. First, we compare the $\sigma(V)$ curves taken from the bright spots along the central and side rows of the (1×2) strands [marked by open and filled, green circles, respectively in Fig. 2(a) and (b)], the region between the central and side rows of the strands (marked by dashed purple lines), and from the trenches between the (1×2) strands (marked by solid purple lines). As shown in Fig. 2d, the $\sigma(V)$ curves taken from the bright spots along the central and side rows of the (1×2) strands are very similar: the intensities of the peaks at -1.5 V and those at -0.7 V are almost identical. As for the $\sigma(V)$ curve taken at the trenches between the strands, although

6

the peak at -0.7 V is very close in intensity to those taken along the central and side rows of the strands, it exhibits a larger peak at -1.5 V. On the other hand, the $\sigma(V)$ curve which is taken in the region between the central and side rows of the strands exhibits a more intense peak at -0.7 V but a less intense peak at -1.5 V. In addition, both filled-state peaks also vary in position by ±0.1 eV depending on their relative populations.

The $\sigma(V)$ curves taken at the brighter and less bright points at the central part of the double-links are shown in Fig. 2e. Both curves have equally intense peaks at -1.5 V. However, at the brighter spots (blue open triangles) a more intense peak is found at -0.7 V. Furthermore, both curves exhibit a peak at +1.1 V in the empty-state region which is not found in any of the $\sigma(V)$ curves taken along the (1×2) strands or at the trenches. This additional peak might account for the brighter appearance of the double-links in the empty-state STM image (Fig. 1b).

The strands on the cross-linked (1×2) reconstruction of rutile $TiO_2(110)$ are occasionally inter-connected by single links, one of which is shown on the right side of Fig. 1b. It is therefore interesting to compare the electronic fingerprints between the two. The $\sigma(V)$ curve taken at the single links (black dashed lines) also exhibits two peaks in the filled-states region with intensities almost equal to the double-links. However, in the single link $\sigma(V)$ the empty-state peak at +1.1 V is absent.

The $\sigma(V)$ curves taken at the corners of the double-links are shown in Fig. 2f. These curves are characterized by two peaks (one at -0.7 V and another -1.5 V) in the filled state region, and a single peak (at +1.1 V) in the empty-state region. Those curves can be divided into three different groups (marked by blue open circles, open squares, and crosses, respectively in Fig. 2f) based on the relative populations of their filled-state peaks, although the cause of this difference is unknown.

We assign the peak at -1.5 V to Ti^{3+} species present on the strands of the cross-linked (1×2) reconstruction in line with the conclusions of Batzill *et al.* [18]. These results are in good agreement with a UPS study by Sánchez-Sánchez *et al.* [16], which found that the Ti^{3+} $3d$ derived gap state located at 1.2 eV BE is only present on the (1×2) reconstructed TiO_2(110) surface.

A peak at, or near -0.7 V has been observed previously from STS measurements of TiO_2(110) and been assigned to O_b-vac states [21-23]. Such species have also been detected in the earlier STS measurement from on top of the simple (1×2) strands [18]. We detect this peak in every region of the image and cannot correlate it with any specific sites. As such, even with atomically-resolved STS, we cannot determine the origin of this peak. The peak could originate from subsurface oxygen vacancies and subsurface interstitial Ti (in line with the conclusions of Sánchez-Sánchez *et al.* [16]), or from the cross-linked (1×2) surface layer itself, or from a combination of the two.

Adsorption at the double-links modifies the electronic structure. As illustrated in Fig. 2e, the $\sigma(V)$ curve taken at the adsorbate covered cross-links (black solid lines) exhibits two peaks in the filled-state region, one at -0.9 V and another at -1.6 V, both shifting to lower energy in comparison to the bare double-links (blue triangles). The appearance of these peaks is also different from the bare double-links. The peak at -1.6 V is significantly broadened and the peak at -0.9 V is significantly less intense. In addition, the peak at +0.9 V is also shifted to lower energy and is much narrower in width.

Cross-linked TiO₂(110)-(1×2) exposure to O₂

Figs. 3a,b display STM images taken from the same area of the cross-linked (1×2) surface before and after an O_2 exposure of 0.01 L (1L = 1.33×10^{-6} mbar.s), performed at 300 K. After O_2 exposure, a number of different species are found at different locations on the surface. These species are marked in Fig. 3c. Bright spots are located at the center of the (1×2) strands (squares), brighter and less bright features are located at the side of the (1×2) strands (solid and dashed circles, respectively), and bright spots between two neighboring cross-links (triangles). In addition, there are a number of double-links that appear much brighter than before O_2 dosing (hexagons).

Since O_2 is reported to dissociate on the (1×2) surface above 200 K [24], we tentatively assign these bright spots to O adatoms. Park *et al.* [25] have studied O_2 adsorption on a $TiO_2(110)$ surface with a (1×1)/(1×2) structure using STM, finding bright spots agglomerated on, or adjacent to individual (1×2) strands. Most of the bright features observed in their study are irregular in shape, some of which elongated along the [001]. In our case, at 0.01 L O_2 exposure, we observe that the bright features that reside at the center of the (1×2) strands have a rather regular shape, with their heights similar to those reported by Park *et al.* [25]. By increasing the O_2 exposure, we observed an increasing number of round-shaped features residing at the center of the (1×2) strands (not shown), suggesting that these are the preferential adsorption sites.

Using UPS we probed the variation in the population of the BGS peak as well as the workfunction, Φ, as a result of O_2 exposure. We first focus on the BGS. As shown in the He I (*hv* = 21.2 eV) UPS spectra (Figs. 3d-e) prior to O_2 exposure, the cross-linked $TiO_2(110)$-(1×2) surface exhibits a BGS peak centered at ~0.9 eV below the E_F, with an intensity much greater than what we measure from the $TiO_2(110)$-

(1×1) surface. Although we could not resolve the BGS peak (at 1.18 eV below the E_F) that arises exclusively from the Ti^{3+} species in the (1×2) strands [16], this enhanced intensity confirms the heavily reduced nature of our cross-linked (1×2) surface.

When O_2 was introduced (as shown in Fig. 3e) at 300 K, the intensity of the BGS peak decreases rather drastically, reducing to half of its original value at a small O_2 exposure of 0.1 L, and then to only ~25 % at 1.0 L. After that, the intensity of the BGS peak decreases at a much slower rate: it still retains ~10 % of its original value following 10 L of O_2 exposure, and can only be totally quenched by 100 L of O_2. The normalized BGS peak intensity is plotted in Fig. 3g as a function of O_2 exposure.

A very similar trend is observed in the workfunction (Φ) measurement. The workfunction, Φ, of the sample is determined using Equation (1), with the E_{kin}^{0} value equal to the kinetic energy onset of the corresponding secondary electron emission spectrum (as indicated by an red arrow in Fig. 3f). Φ is plotted against O_2 exposure in Fig. 3f. Without any O_2 exposure, the surface has a Φ value of 4.67 eV. In the regime of small O_2 exposure ($\leq$ 2 L), Φ increases rather quickly, reaching 4.91 eV at 0.2 L O_2, then 4.95 eV at 2 L O_2. After that, Φ varies only slightly with increasing O_2 exposure, reaching a value of 5.03 eV at 100 L O_2. The increase in the surface workfunction observed on the (1×2) reconstructed surface here is very similar to that measured on the TiO_2(110)-(1×1) by Borodin et al. [26], who, using metastable impact electron spectroscopy (MIES) and UPS, found that the workfunction of the reduced TiO_2(110)-(1×1) surface increases by 0.15 eV after oxidation. Also, as pointed out by Onda et al. [27], the workfunction of as-prepared TiO_2(110)-(1×1) can vary between surface preparation .

Since both the workfunction and the intensity of the BGS peak of the surface vary with O_2 exposure, we plotted the Φ against the BGS intensity (green) in Fig. 3g. The workfunction of the surface increases linearly with decreasing intensity of the BGS peak. As the change in the workfunction reflects, to an extent, the number of O atoms adsorbed on the surface, the linear relationship reveals that when an O atom adsorbs on the (1×2) strand, it will withdraw the excess electrons from it, causing a reduction in the BGS population.

Conclusions

By performing STS in the CITS mode at 78 K, we demonstrated that the cross-linked $TiO_2(110)$-(1×2) surface is characterized by two states in the band gap, located at 0.7 and 1.5 eV below E_F. The populations of these two states vary differently across different parts of the (1×2)-reconstructed surface. We also showed that when O adatoms are adsorbed on the cross-linked $TiO_2(110)$-(1×2) surface, it withdraws excess electrons from the substrate, causing a decrease in the BGS population, and an increase in the workfunction.
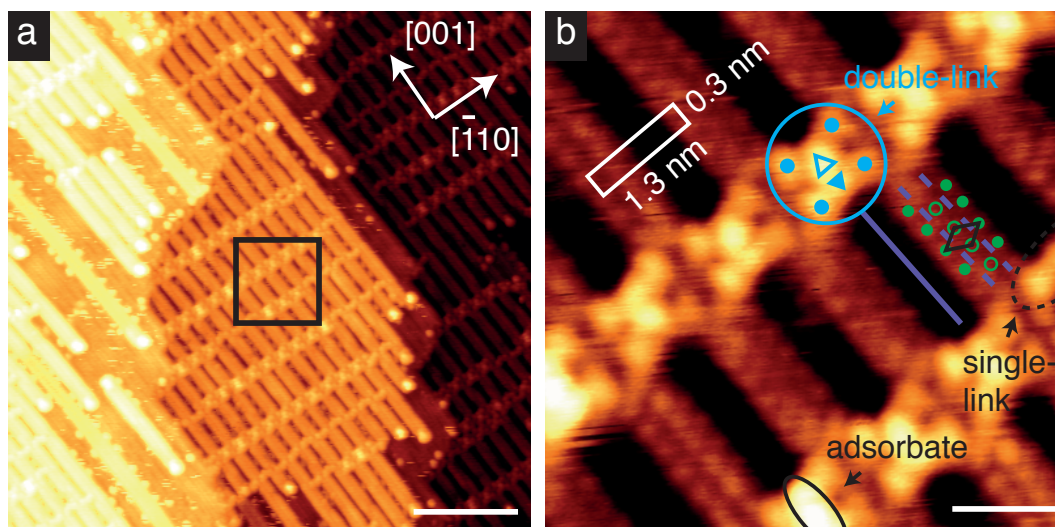
Fig 1. **(a)** 39×39 nm^2 STM image of the cross-linked TiO$_2$(110)-(1×2) surface, recorded at 78 K. Scale bar = 7.8 nm. **(b)** Atomically resolved STM image (6×6 nm^2, 0.9 V, 0.1 nA) taken from the region marked by the square in (a). Scale bar = 1.2 nm. Green filled and open circles mark the bright spots along the side and central rows of a (1×2) strand, respectively. A double-link is circled blue: blue open and solid triangles mark the brighter and less-bright spots at the center, and blue circles mark the corners. Solid purple lines mark the trenches between neighboring (1×2) strands; purple dashed lines mark the dark regions between the atomic rows on the (1×2) strands. A dashed black oval marks a single-link. A solid black oval marks the cross-link that is bonded to an adsorbate.
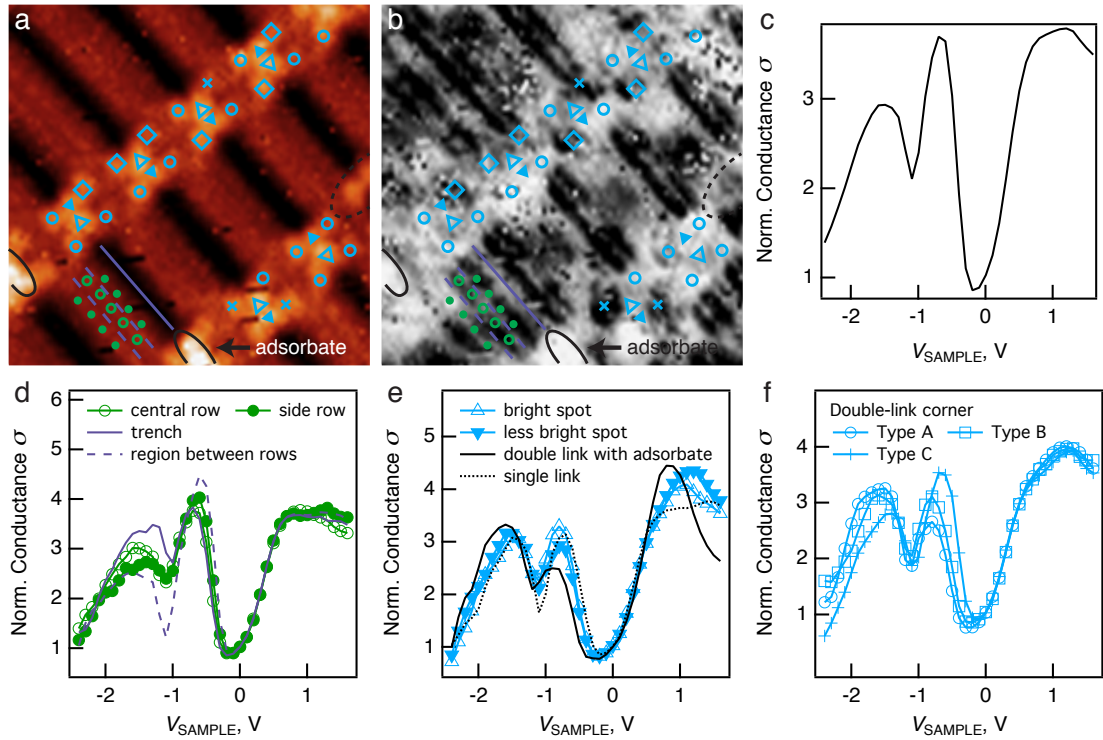
Fig. 2. (a) 6×6 nm² topographical STM image recorded during CITS measurement at 78 K (scan parameters: V_{SAMPLE} = 0.9 V, I_T = 0.15 nA). **(b)** The corresponding tunneling current (I_T) map at -0.7 V, recorded during CITS. In a,b, green solid and open circles mark the bright spots on the side and central rows of the (1×2) strands respectively. Blue open and solid triangles mark the brighter and less bright spots at the double-link centers. Blue open circles, open squares and crosses mark the bright spots at their corners. Purple solid lines mark trenches between the (1×2) strands, and purple dashed lines mark the dark region between the atomic rows on the strands. Black dashed lines mark single-links. Black ovals mark adsorbates (probably H_2O). adsorbed on the cross-links. **(c)** The normalized conductance curve, σ(V), which is averaged across the whole surface area of the image in (a). **(d-f)** Normalized conductance curves, σ(V), recorded from different features on the cross-linked (1×2) reconstruction. (d) Bright spots on the side and central rows on the (1×2) strands (green solid and open circles, respectively), the region between the atomic rows on the strands (purple dashed line), and the trenches between strands (purple solid line).

13

(e) Brighter and less bright spots (blue open and solid triangles, respectively) at the central part of the double-links, single links (black dashed line) and the double-links bonded to an adsorbate (black solid line). (f) Double-link corners, which can be divided into three groups (blue open circles, open squares and crosses respectively) based on their difference in their $\sigma(V)$ curves.
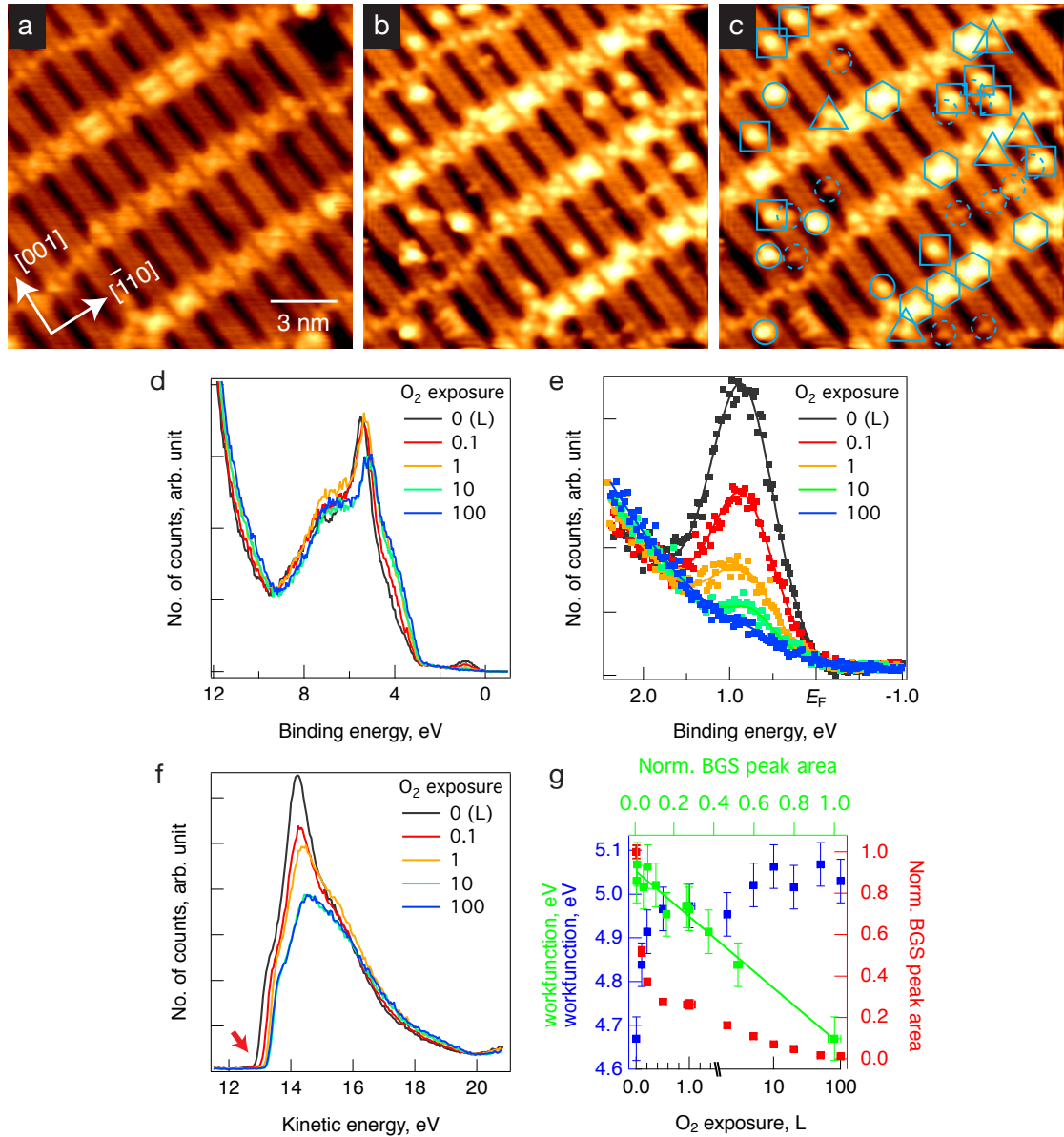
Fig. 3. (a-b) STM images of the cross-linked TiO$_2$(110)-(1×2) surface, recorded before (a) and after (b) O$_2$ exposure of 0.01 L at 300 K (15×15 nm^2, 1.2 V, 20 pA). **(c)** As (b), overlaid with feature markers: squares mark the bright features located at the center of the (1×2) strands, solid and dashed circles mark the brighter and less bright features located at the side of the strands, respectively, triangles mark the bright features nearby the corners of two neighboring cross-links, hexagons mark the cross-links that become much brighter after O$_2$ exposure. **(d)** He I (*hv* = 21.2 eV) UPS of the cross-linked TiO$_2$(110)-(1×2) surface taken as a function of O$_2$ exposure at 300 K. **(e)** The corresponding spectra recorded in the region of the BGS peak (B.E. ≈ 1 eV).

(f) The corresponding secondary electron emission spectra. The red arrow indicates the kinetic energy *onset*, E_{kin}^{0}. **(f)** Workfunction (Φ, blue) and the normalized area of the BGS peak (A_{BGS}, red) of the cross-linked $TiO_2(110)$-(1×2) surface plotted as a function of O_2 exposure, and the resultant plot of Φ versus A_{BGS} (green), revealing a linear relationship between the two.

References

[1]   U. Diebold, Surf. Sci. Rep. 48 (2003) 53.

[2]   M.A. Henderson, Surf. Sci. Rep. 66 (2011) 185.

[3]   C.L. Pang, R. Lindsay, G. Thornton, Chem. Rev. 113 (2013) 3887.

[4]   M. Blanco-Rey, J. Abad, C. Rogero, J. Mendez, M. Lopez, J. Martin-Gago, P. de Andres, Phys. Rev. Lett. 96 (2006) 055502.

[5]   R.A. Bennett, P. Stone, N.J. Price, M. Bowker, Phys. Rev. Lett. 82 (1999) 3831.

[6]   H.H. Pieper, K. Venkataramani, S. Torbrügge, S. Bahr, J.V. Lauritsen, F. Besenbacher, A. Kühnle, M. Reichling, Phys. Chem. Chem. Phys. 12 (2010) 12436.

[7]   M. Li, W. Hebenstreit, U. Diebold, Phys. Rev. B 61 (2000) 4926.

[8]   H. Onishi, Y. Iwasawa, Surf. Sci. 313 (1994) L783.

[9]   M. Blanco-Rey, J. Abad, C. Rogero, J. Mendez, M. Lopez, E. Román, J. Martin-Gago, P. de Andres, Phys. Rev. B 75 (2007) 081402.

[10]   K. Park, M. Pan, V. Meunier, E.W. Plummer, Phys. Rev. Lett. 96 (2006) 226105.

[11]   N. Shibata, A. Goto, S.Y. Choi, T. Mizoguchi, S.D. Findlay, T. Yamamoto, Y. Ikuhara, Science 322 (2008) 570.

[12]   S. Takakusagi, K.-I. Fukui, F. Nariyuki, Y. Iwasawa, Surf. Sci. 523 (2003) L41.

[13]   C.L. Pang, S.A. Haycock, H. Raza, P.W. Murray, G. Thornton, O. Gülseren, R. James, D.W. Bullett, Phys. Rev. B 58 (1998) 1586.

[14]   Q. Wang, A.R. Oganov, Q. Zhu, X.-F. Zhou, Phys. Rev. Lett. 113 (2014) 266101.

[15]   R. Patel, J. Vac. Sci. Technol. A 15 (1997) 2553.

[16]   C. Sánchez-Sánchez, M.G. Garnier, P. Aebi, M. Blanco-Rey, P.L. de Andres, J.A. Martín-Gago, M.F. López, Surf. Sci. 608 (2013) 92.

[17]   P. Murray, N. Condon, G. Thornton, Phys. Rev. B Condens. Matter 51 (1995) 10989.

[18]   M. Batzill, K. Katsiev, D. Gaspar, U. Diebold, Phys. Rev. B 66 (2002) 235401.

[19]   A. Visikovskiy, K. Mitsuhara, Y. Kido, J. Vac. Sci. Technol. A 31 (2013) 061404.

[20]   R.M. Feenstra, J.A. Stroscio, A.P. Fein, Surf. Sci. 181 (1987) 295.

[21]   T. Minato, Y. Sainoo, Y. Kim, H.S. Kato, K.-I. Aika, M. Kawai, J. Zhao, H. Petek, T. Huang, W. He, B. Wang, Z. Wang, Y. Zhao, J. Yang, J.G. Hou, J. Chem. Phys. 130 (2009) 124502.

[22]   A.C. Papageorgiou, N.S. Beglitis, C.L. Pang, G. Teobaldi, G. Cabailh, Q. Chen, A.J. Fisher, W.A. Hofer, G. Thornton, Proc. Natl. Acad. Sci. USA 107 (2010) 2391.

[23]   M. Setvin, C. Franchini, X. Hao, M. Schmid, A. Janotti, M. Kaltak, C.G. Van de Walle, G. Kresse, U. Diebold, Phys. Rev. Lett. 113 (2014) 086402.

[24]   J. Abad, C. Sánchez-Sánchez, P. Vilmercati, A. Goldoni, M.F. López, J.A. Martín-Gago, Vacuum 85 (2011) 1056.

[25]   K. Park, M. Pan, V. Meunier, E.W. Plummer, Phys. Rev. B 75 (2007) 245415.

[26]   A. Borodin, M. Reichling, Phys. Chem. Chem. Phys. 13 (2011) 15442.

[27]   K. Onda, B. Li, H. Petek, Phys. Rev. B 70 (2004) 045415.